JOURNAL OF BIOSCIENCE AND BIOENGINEERING
Vol. 98, No. 5, 338–343. 2004

Acidophilic Xylanase from *Aureobasidium pullulans*: Efficient Expression and Secretion in *Pichia pastoris* and Mutational Analysis

HIDENORI TANAKA,[1] TOMOKO OKUNO,[1] SATOSHI MORIYAMA,[1] MICHIO MUGURUMA,[1] AND KAZUYOSHI OHTA[1]*

Department of Biochemistry and Applied Biosciences, Faculty of Agriculture, University of Miyazaki, 1-1 Gakuen Kibanadai Nishi, Miyazaki 889-2192, Japan[1]

Received 8 June 2004/Accepted 4 August 2004

A yeast-like fungus *Aureobasidium pullulans* var. *melanigenum* strain ATCC 20524 produces an extracellular acidophilic endo-1,4-β-xylanase with an optimum pH of 2.0 [Ohta *et al.*, J. Biosci. Bioeng., 92, 262–270 (2001)]. The *xynI* cDNA encoding the precursor protein (XynI) was expressed in the methylotrophic yeast *Pichia pastoris* under the control of the alcohol oxidase I gene promoter. The 34 amino acid prepro-signal peptide of the *A. pullulans* XynI directed the efficient secretion of 178 mg of active xylanase per liter of the culture medium. The secretion level of the xylanase with its own signal peptide was comparable to that of the mature protein fused to the prepro leader from *Saccharomyces cerevisiae* α-mating factor and twofold higher than that of the mature protein fused to the pre-type signal peptide from *P. pastoris* acid phosphatase. The N-terminal amino acid sequence and the apparent M_r of 24 kDa of the secreted recombinant protein indicated the native-like processing of the *A. pullulans* XynI signal sequence in *P. pastoris*. The three-dimensional model and mutational analysis of the *xynI* gene product showed that Asp-73 and Glu-157 residues located at the upper and lower edges of the active site cleft, respectively, play a significant role in its low pH optimum.

[**Key words:** acidophilic enzyme, *Aureobasidium pullulans*, heterologous expression, *Pichia pastoris*, protein secretion, signal sequence, site-directed mutagenesis, xylanase]

β-1,4-Xylan is a major component of hemicellulose in the cell walls of monocots and hard woods (1). Xylanolytic enzymes are valuable for applications in the pulp and paper, textile, and food industries and in agriculture (2). Endo-1,4-β-xylanases (1,4-β-D-xylan xylanohydrolase; EC 3.2.1.8) hydrolyze the internal β-1,4-xylosidic linkages in the xylan backbone to produce short-chain xylooligosaccharides. Xylanases have been classified into two glycosyl hydrolase families 10 (F) and 11 (G) based on amino acid sequence similarities (http://afmb.cnrs-mrs.fr/CAZY/): family-11 xylanases with a M_r of about 20 kDa and family-10 xylanases with a M_r of about 35 kDa (3, 4).

We have previously shown that a yeast-like fungus *Aureobasidium pullulans* var. *melanigenum* strain ATCC 20524 produces an extracellular acidophilic xylanase with an optimum pH of 2.0 (5). The *A. pullulans* enzyme is a family-11 xylanase with a M_r of 24 kDa. The xylanase gene (*xynI*) encoded a precursor protein (XynI) composed of a putative prepro-signal peptide of 34 amino acids and a mature protein of 187 amino acids. The *xynI* cDNA was expressed in the yeast *Saccharomyces cerevisiae* and its product was secreted by its own signal peptide into the culture medium (5). Li and Ljungdahl (6) demonstrated that the signal peptide of the equivalent xylanase XynA from *A. pullulans* strain Y-2311-1 was more efficient than the pre-signal peptides of *S. cerevisiae* invertase and α-mating factor (α-MF) in secreting the heterologous xylanase from *S. cerevisiae*.

The methylotrophic yeast *Pichia pastoris* has several advantages over *S. cerevisiae* as a host system for heterologous expression because of its high secretion efficiency, high cell densities attained in inexpensive culture media, and the relative ease of scale-up to industrial processes (7). Berrin *et al*. (8) reported that an *Aspergillus niger* family-11 xylanase was efficiently secreted from *P. pastoris* using the *S. cerevisiae* invertase signal peptide. We describe here the functional expression of the *A. pullulans* XynI in *P. pastoris* and the high-level secretion by the XynI signal peptide. Furthermore, the three-dimensional (3D) model and mutational analysis of the acidophilic xylanase have facilitated identification of key amino acid residues responsible for its low pH optimum, along with their locations.

* Corresponding author. e-mail: k.ohta@cc.miyazaki-u.ac.jp
phone/fax: +81-(0)985-58-7217

Abbreviations: *AOX1*, alcohol oxidase I gene; 3D, three-dimensional; α-MF, α-mating factor; PHO1, acid phosphatase; YNB, yeast nitrogen base.

MATERIALS AND METHODS

Yeast strain and plasmids The yeast *P. pastoris* strain GS115 (*his4*) and the integrative expression vectors pPIC3.5, pHIL-S1,

and pPIC9 were obtained from Invitrogen (Carlsbad, CA, USA). These yeast expression vectors contain the promoter and terminator of the alcohol oxidase I gene (*AOX1*) as an expression cassette and the *HIS4* selectable marker. Vectors pHIL-S1 and pPIC9 have signal sequences from *P. pastoris* acid phosphatase (PHO1) and *S. cerevisiae* α-MF, respectively, while pPIC3.5 does not contain a secretion signal.

DNA manipulations and analyses Restriction endonucleases and DNA-modifying enzymes were used as recommended by the supplier (Nippon Gene, Tokyo). Standard molecular cloning techniques were performed as described by Sambrook and Russell (9). PCRs were done in a thermal cycler (GeneAmp PCR system 2400; PE Applied Biosystems, Foster City, CA, USA). The nucleotide sequences were determined using an automated DNA sequencer ABI Prism 310 Genetic Analyzer (PE Applied Biosystems).

Construction of yeast expression plasmids A full-length cDNA of the xylanase gene *xynI* from *A. pullulans* strain ATCC 20524 was previously cloned into pUC18 (5). The *xynI* cDNA was used for construction of the following series of yeast expression plasmids.

Plasmids containing the three different secretion signals On the basis of the nucleotide sequence of *xynI* (5), the following PCR primers were designed to amplify the precursor or mature protein region of *xynI* cDNA (letters in bold type indicate the *xynI* coding sequence): 5′-CGGAATTCCGAAC**ATGAAGTTCTTCGCCAC TATT**-3′ (P1 forward) and 5′-CGGAATTCCGTGACATCTA**AGA GACAGTAACGCT**-3′ (P2 reverse) containing *Eco*RI sites (underlined) for expression of the precursor protein with its own signal sequence using pPIC3.5; 5′-CCGGAATTC**GCCGGCCCCG GTGGCATCAACTAC**-3′ (P3 forward) and 5′-TCCCCCGGGG-GATGACATCTA**AGAGACAGTAACGCT**-3′ (P4 reverse) containing *Eco*RI and *Sma*I sites (underlined) for fusion of the PHO1 signal peptide encoded in pHIL-S1 to the mature protein; and the P3 forward and P2 reverse primers for fusion of the α-MF signal peptide encoded in pPIC9 to the mature protein. These three amplified *xynI* cDNA fragments were digested with the appropriate endonucleases and cloned into pPIC3.5, pHIL-S1, and pPIC9 to yield pXYN119, pXYN118, and pXYN120, respectively.

Mutant plasmids Site-directed mutagenesis was performed using the overlap extension PCR method as described previously (10). The following internal mutagenic primers were designed to incorporate mutations (in bold type): D73N forward, 5′-CAGCGG C**A**ACTTCGTCGTCG-3′; D73N reverse, 5′-GT**T**GCCGCTGAC GCCGTTGG-3′; E153T forward, 5′-CACCGAC**ACT**CGCGTCA ATG-3′; E153T reverse, 5′-**AGT**GTCGGTGCAGACGGTGTA-3′; E157Q forward, 5′-CGCGTCAAT**C**AGCCTTCCAT-3′; E157Q reverse, 5′-**G**ATTGACGCGCTCGTCGGTG-3′; V141C forward, 5′-TACCGTC**TG**CAGCGATGGCG-3′; V141C reverse, 5′-CATC GCTG**CA**GACGGTACCG-3′; C150Y forward, 5′-CACCGTCT**A** CACCGACGAGC-3′; and C150Y reverse, 5′-CGTCGGTG**T**AGA CGGTGTAG-3′.

For the first-round PCR, the P1 forward or P2 reverse external primer (see above) was used along with equimolar amounts of reverse or forward internal mutagenic primer, respectively. Mutated fragments were amplified using *xynI* cDNA as a template, DNA polymerase (KOD -Plus-; Toyobo, Osaka) and dNTPs through 25 cycles of denaturation (15 s at 94°C), annealing (30 s at 56°C), and extension (1 min at 68°C). Two amplified fragments having overlapping ends were precipitated by ethanol, redissolved, and combined. Subsequent 3′ extension of the complementary strand consisted of a denaturation step at 94°C for 2 min and five cycles of the following steps: denaturation (15 s at 94°C), annealing of the denatured fragments at the overlap (30 s at 60°C), and extension (1 min at 68°C). The mutant fusion product was gel-purified using the QIAquick gel extraction kit (Qiagen, Valencia, CA, USA). Each purified product was amplified further by the second-round PCR using the P1 forward and P2 reverse primers. The amplified fragments, each carrying mutation that corresponded to D73N, V141C/C150Y, E153T, and E157Q, were digested with *Eco*RI and cloned into pPIC3.5 to yield pXYN128, pXYN129, pXYN131, and pXYN132, respectively. Sequences of the mutant plasmids were verified by DNA sequence analysis of the entire inserts.

Plasmid containing XynI pre-signal sequence To delete the 18-amino acid pro-region from the XynI prepro-signal sequence (see Fig. 1A), overlap extension was performed using the following internal primers: P5 forward (5′-AGCCGTCGCTGCCGGCC CCG-3′) and P6 reverse (5′-CGGGGCCGGCAGCGACGGCT-3′) that are complementary to each other and correspond to the sequence at the pre-region (underlined) and mature XynI boundary. The amplified fragment was cloned into pPIC3.5 to yield pXYN123.

Transformation of *P. pastoris* The resulting plasmids were linearized by digestion with *Sac*I to favor integration via homologous recombination at the *AOX1* locus. These DNA segments were used to transform the yeast *P. pastoris* strain GS115 by electroporation with a Bio-Rad Gene Pulser II (Hercules, CA, USA) according to the manufacturer's instructions. As the corresponding controls, yeast cells were also transformed with the vector pPIC3.5, pHIL-S1, or pPIC9 using the same method. His^+ transformants were recovered on MD plates (13.4 g of yeast nitrogen base [YNB] w/o amino acids [Sigma Chemical, St. Louis, MO, USA], 4 μg of biotin, 20 g of dextrose, 15 g of agar, per liter). A representative transformant for each construct was selected for xylanase production in shake-flask cultures.

Media and culture conditions for *P. pastoris* transformants *P. pastoris* transformants were inoculated into 20 ml of BMG medium (13.4 g of YNB, 4 μg of biotin, 10 g of glycerol, per liter of 100 mM potassium phosphate buffer [pH 6.0]) in 100-ml Erlenmeyer flasks. The pre-cultures were grown on an orbital shaker (150 rpm) at 30°C to an OD_{600} of 1.3 to 1.6. The cells were harvested by centrifugation at 1500×*g* for 10 min and resuspended in 100 ml of BMMY medium (the same as BMG, except that glycerol was replaced by methanol [5 ml/*l*] and the medium was supplemented with yeast extract [10 g/*l*] and peptone [20 g/*l*]) in 500-ml Erlenmeyer flasks. The cultures were grown at 30°C under the same aerobic conditions. To enable methanol induction of the *AOX1* promoter, 0.5 ml of methanol was fed every 24 h during the culture period. The growth of transformants was monitored by measuring the OD_{600} periodically. Culture aliquots (1 ml) were collected daily and cells were removed by centrifugation at 10,000×*g* for 10 min. The supernatant fluids were assayed for the xylanase activity as described below.

Enzyme and protein assays The reaction mixture consisted of 0.5 ml of a 1.0% (w/v) suspension of oat-spelt xylan (Sigma) in deionized water and 0.5 ml of a suitably diluted enzyme solution in 0.1 M sodium acetate–HCl buffer (pH 2.0). After incubation at 45°C for 30 min, reducing sugars were determined by the dinitrosalicylic acid method (11). One unit (U) of xylanase activity was defined as the amount of enzyme that liberated 1 μmol of xylose equivalents from xylan per minute. Protein was measured by the method of Lowry *et al*. (12) with BSA (Sigma) as the standard.

Enzyme purification The transformant cultures grown for 5 d were centrifuged at 4000×*g* for 25 min at 4°C. Clear supernatant (200 ml) was concentrated to 35 ml by ultrafiltration through a 3×10^3 molecular-weight cut-off membrane (Diaflo YM3; Amicon, Beverly, MA, USA) in a stirred cell. The concentrated sample was loaded onto a Q-Sepharose HP (Amersham Biosciences, Piscataway, NJ, USA) column (1.6×20 cm) that was equilibrated with 20 mM acetate buffer (pH 6.0). The adsorbed enzyme was eluted at a flow rate of 1.0 ml/min with a linear gradient of 0 to 0.5 M NaCl in the same buffer. The fractions exhibiting enzyme activity were pooled and then chromatographed on a Superdex 75 pg (Amer-

A

```
Apm XynI     1 MKFFATIAALVVAAVAAPVAEADAEASSPMLIERAGPGGI  40
                    pre-region      pro-region
Ap XynA      1 MKFFATIAALVVGAVAAPVAEAEAEASSPMLIERAGPGGI  40
Ang XynI     1 MKVTAAFAGLLVTAFAAPVPE-------PVLVSRS--AGI  31
Ak XynC      1 MKVTAASAGLLGHAFAAPVPQ-------PVLVSRS--AGI  31
               **. *: *.*:  *.****.:       *:*:.*:  .**
```

B

```
Apm XynI   137 LGTVVSDGATYTVCTDERVNEPSITGTSTFKQYWSVRQTK 176
Ap XynA    137 LGTVCSDGATYTVYTDTRTNQPSITGTSTFKQYWSVRQTK 176
Ang XynI   125 LGTVYSDGSTYQVCTDTRTNEPSITGTSTFTQYFSVREST 164
Ak XynC    125 LGTVYSDGSTYQVCTDTRTNEPSITGTSTFTQYFSVREST 164
                **** ***:** * ** *.*:**********.**:***::.
```

FIG. 1. Alignment of N-terminal (A) and internal (B) amino acid sequences of *A. pullulans* var. *melanigenum* XynI and homologous xylanases. Apm, *A. pullulans* var. *melanigenum*; Ap, *A. pullulans*; Ang, *A. niger*; Ak, *A. kawachii*. The alignment was done using the CLUSTAL W program. Dashes indicate gaps introduced during the alignment process. Asterisks indicate identity, and single and double dots indicate semiconservative and conservative replacements, respectively. The signal peptides are underlined. Putative recognition sites for the signal peptidase and *KEX2*-like endopeptidase in the XynI signal peptide are shown by open and solid arrowheads, respectively. The boxed residues in XynI indicate the sites for targeted mutagenesis to be used in this study.

sham Biosciences) column (1.6×60 cm) at a flow rate of 1.0 ml/min with 10 mM acetate buffer (pH 6.0) containing 0.15 M NaCl. The recombinant xylanase was eluted as a single protein peak that coincided with the peak of enzyme activity.

Effect of pH and temperature The effects of pH and temperature on the xylanase activity of the recombinant enzyme and its variants were determined as previously described for the native enzyme (5).

SDS–PAGE and N-terminal amino acid sequencing SDS–PAGE was done according to the method of Laemmli (13). Gels were stained for protein with Coomassie Brilliant Blue R-250. The protein bands were electroblotted onto a polyvinylidene membrane (Bio-Rad) as described previously (14). The N-terminal amino acid sequence was identified using a G1005A Hewlett-Packard protein sequencer (Palo Alto, CA, USA).

Amino acid numbering The standard amino acid numbering used in the text starts at the N-termini of the precursor proteins (see Fig. 1).

RESULTS AND DISCUSSION

Effect of signal sequences on secretion levels of recombinant xylanase from *P. pastoris* The efficiency of xylanase secretion directed by the XynI signal peptide in *P. pastoris* was compared with those directed by the two yeast signal peptides from *P. pastoris* PHO1 and *S. cerevisiae* α-MF that were fused to the mature XynI protein. The 34 amino acid prepro-signal peptide of the *A. pullulans* XynI contains a putative recognition site for a signal peptidase in the endoplasmic reticulum and a processing site for a *KEX2*-like endopeptidase in the Golgi apparatus (Fig. 1A). The 89 amino acid prepro leader of *S. cerevisiae* α-MF consists of a 19 amino acid pre-signal sequence, a 66 amino acid pro-sequence and the repeats of spacer peptide (EAEA). However, the 22 amino acid signal peptide of the PHO1 lacks the pro-region. Three transformants showed similar growth curves, independent of the secretory signal contained (Fig. 2A). The three transformants secreted recombinant xylanases by signal peptides of *A. pullulans* XynI, *P. pastoris* PHO1, and *S. cerevisiae* α-MF during the 5 d of induction by methanol, and xylanase activities in the culture supernatants were 38, 15, and 38 U/ml, respectively (Fig. 2B). Control cells transformed with the corresponding vector plasmids were devoid of the extracellular enzyme activity (data not shown). On the basis of the specific activities of the purified enzymes (see below), the estimated concentrations of the recombinant xylanases in the culture medium were 178 mg/*l* for XynI, 180 mg/*l* for α-MF, and 100 mg/*l* for PHO1. Thus, the amount of recombinant xylanase secreted into the medium by the XynI signal peptide was comparable to that by the prepro leader of α-MF and two-fold higher than that by the PHO1 pre-type signal peptide, and was also higher than 60 mg/*l* previously reported for the *A. niger* xylanase secreted from *P. pastoris* using the 19 amino acid signal peptide of the *S. cerevisiae* invertase (8).

Purification and properties of recombinant xylanase Recombinant enzyme was purified from the culture supernatant after the *P. pastoris* transformant bearing the XynI signal peptide was grown for 5 d. The recovery yield was as high as 27.9%, and the specific activity was 213 U/mg, which was lower than that of the native enzyme (512 U/mg) (5), probably because of incorrect post-translational modifi-

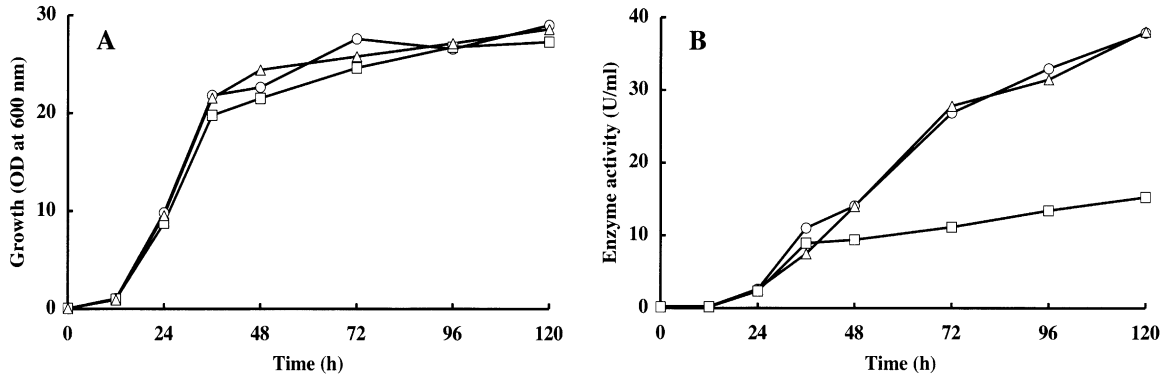

FIG. 2. Growth (A) and extracellular xylanase production (B) in shake-flask cultures of *P. pastoris* transformants. The *P. pastoris* transformants were grown at 30°C in the buffered methanol complex medium. The values represent the means of three independent experiments. Symbols: circles, XynI signal peptide; squares, PHO1 signal peptide; triangles, α-MF signal peptide.

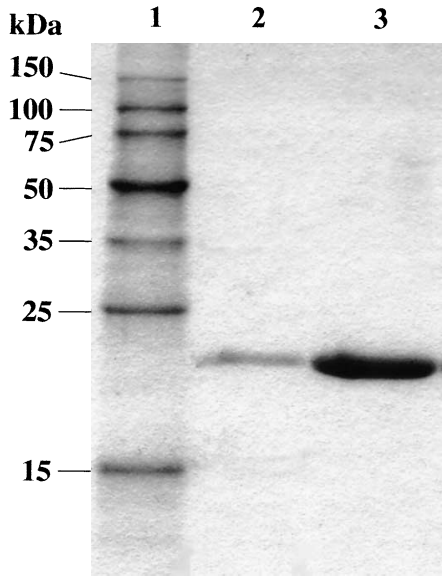

FIG. 3. SDS–PAGE analysis of purified native and recombinant xylanases. SDS–PAGE was done using a 12.5% (w/v) polyacrylamide slab gel. Protein was stained by Coomassie Brilliant Blue R-250. Lanes: 1, standard proteins; 2, the native xylanase; 3, the recombinant xylanase.

cations. The specific activities of the other two recombinant xylanases purified for comparison were 210 U/mg for α-MF and 150 U/mg for PHO1. Analysis by SDS–PAGE of the purified recombinant xylanase revealed a single band with a M_r of 24 kDa, which was similar to that of the native enzyme purified from the culture filtrate of *A. pullulans* (Fig. 3). It is probable that the recombinant enzyme is *O*-linked glycosylated since there was no putative *N*-linked glycosylation site in the deduced amino acid sequence of *A. pullulans* XynI (5). To confirm the two step processing of the XynI prepro-signal sequence, the XynI without the pro-sequence was also expressed in the pXYN123 transformant. The N-terminal amino acid sequences of recombinant enzymes secreted from *P. pastoris* transformants bearing the XynI prepro-signal sequence and only the pre-signal sequence were both determined to be AGPGGIN, which is identical to that of the native enzyme (5). The results show that both the pre- and pro-signal peptides of *A. pulllulans* XynI were correctly recognized and processed by the *P. pastoris* secretory pathway.

The recombinant enzyme showed maximal activity at pH 2.5, and the pH-activity profile was similar to that of the native enzyme with an optimum pH of 2.0 (Fig. 4A). The temperature-activity profile of the recombinant enzyme shifted from that of the native enzyme to a temperature lower by 10 units, and the optimum temperature of the recombinant enzyme was 40°C (Fig. 4B).

Structural prediction of XynI *A. pullulans* XynI showed 66% sequence identity to acidophilic xylanases, *A. niger* xylanase I and *Aspergillus kawachii* xylanase C (XynC), for which 3D structures were available (15, 16). Based on the common sequence pattern between *A. pullulans* XynI and the *Aspergillus* enzymes, we generated a plausible 3D model for the *A. pullulans* XynI protein using Swiss-Model (17–19) (Fig. 5). The overall structure of the XynI has the shape of a right hand in common with family-11 xylanases (15, 16, 20) and is composed of the fingers at the top, the palm at the right-hand side, and the thumb at the bottom of the molecule. The active site was located within an extended open cleft, which is lined with many aromatic residues and is large enough to accommodate the xylan polymers. The two conserved glutamate residues, Glu-114 and -208, which could be involved in catalysis as a nucleophile and an acid-base catalyst, respectively, extend their side chains to the bottom of the cleft from the opposite sides. Some aromatic residues forming subsites were also suggested to be structural features among acidophilic xylanases (16).

Mutational analysis of amino acid residues potentially responsible for the low pH optimum of xylanase

Conserved Asp residue in xylanases with low pH optima An Asp-64 residue of the *A. niger* xylanase I is suggested to be critical for its low pH optimum of 3.0 (15). Subsequent studies of the *A. kawachii* XynC by X-ray crystallography and site-directed mutagenesis showed the importance of the equivalent Asp-64 residue in the low pH optimum of 2.0 (16). Availability of the *P. pastoris* expression system and the 3D structure of the *A. pullulans* xylanase allowed us to

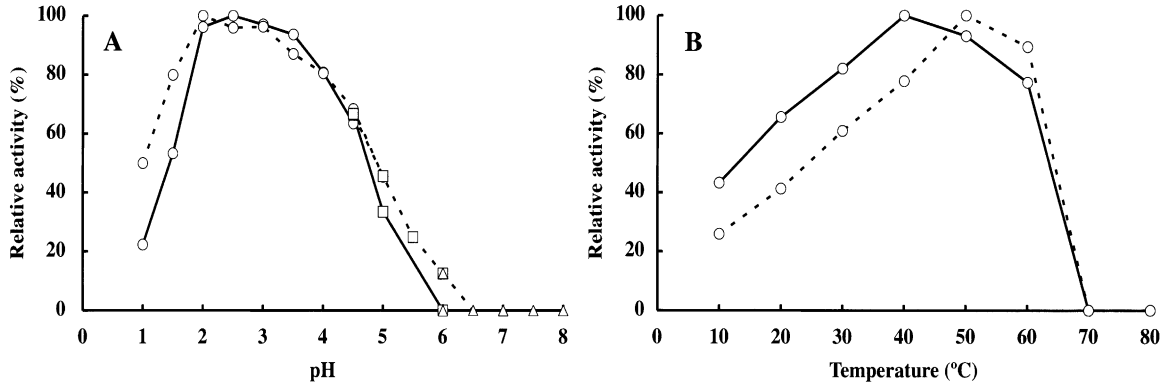

FIG. 4. Effect of pH (A) and temperature (B) on the enzyme activity of recombinant xylanase. The broken lines indicate the previous data of the native enzyme (5). Relative activity was expressed as percentage of the highest activity. The values represent the means of three measurements. (A) The enzyme activity was determined using 0.1 M sodium acetate–HCl (pH 1.0 to 4.5), 0.1 M acetate (pH 4.5 to 6.0), and 0.1 M phosphate (pH 6.0 to 8.0) buffers. (B) The enzyme activity was determined using various temperatures at pH 2.0.

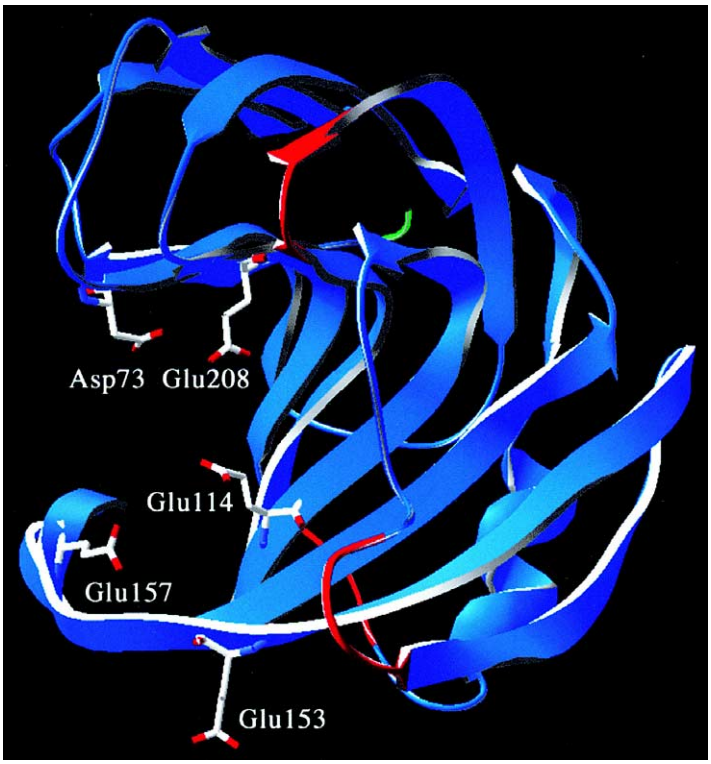

FIG. 5. Hypothetical 3D structure proposed for *A. pullulans* XynI protein. The ribbon diagram was created on the basis of its homology with the structures of *Aspergillus* xylanases using the Swiss-Model server and DeepView software.

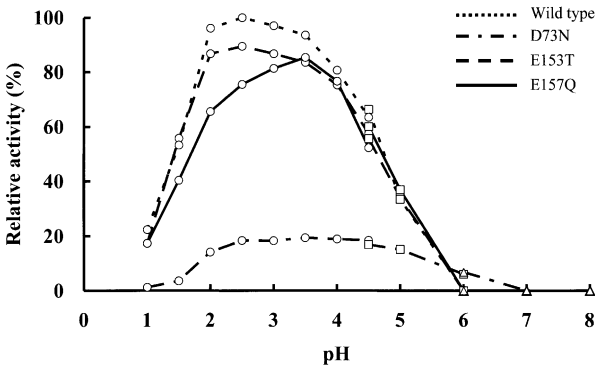

FIG. 6. Effect of pH on the enzyme activities of the mutant xylanases. The values correspond to the averages of three measurements. The enzyme activity was determined using 0.1 M sodium acetate–HCl (pH 1.0 to 4.5), 0.1 M acetate (pH 4.5 to 6.0), and 0.1 M phosphate (pH 6.0 to 8.0) buffers. Relative activity was expressed as a percentage of the highest activity of the recombinant wild-type enzyme (see Fig. 4A).

determine whether the corresponding Asp-73 residue is responsible for the acidophilicity by means of site-directed mutagenesis and to map its position at the upper edge of the active site cleft (see Fig. 5). The activity of the D73N variant decreased to about 19% of that of the wild-type XynI and its optimum pH shifted upward (Fig. 6); it is likely that the asparagine residue of the D73N variant maintains the hydrogen bond with the acid-base catalyst Glu-208 and this interaction prevents the proton of Glu-208 from dissociating as described for the *A. kawachii* XynC (16).

Amino acid residues substituted between A. pullulans XynI and XynA The amino acid sequences of XynI (5) and the equivalent xylanase XynA from *A. pullulans* strain Y-2311-1 (21) differ in 10 out of 187 residues. Despite the high sequence similarity, the *A. pullulans* XynA displays a higher optimal pH of 4.8 (22). Among the 10 amino acid substitutions in XynI *ver* XynA, the four residues at positions 141 (Val *ver* Cys), 150 (Cys *ver* Tyr), 153 (Glu *ver* Thr), and 157 (Glu *ver* Gln) (Fig. 1B) were hypothesized to be responsible for its lower pH optimum on the basis of their positions in the 3D structure described above. Accordingly, we constructed three mutant plasmids, pXYN129 (V141C/C150Y), pXYN131 (E153T), and pXYN132 (E157Q). The E153T and E157Q variants secreted from *P. pastoris* were enzymatically active, but not the double mutant V141C/C150Y probably due to misfolding and aggregation (data not shown). While the optimum pH of the E157Q variant shifted to 3.5, the variant retained the full activity of the wild-type enzyme (Fig. 6). These results showed that Glu-157 partially determines the pH dependence of activity by a different action from that of Asp-73; the Glu-157 residue located in the thumb at the bottom and pointing into the active site is protonated at low pH, so that electrostatic repulsion would disappear between the cleft and the xylan that exhibits a certain degree of negative charge due to glucuronic acid substituents. The E157Q variant showed enzyme activity in the higher pH range, probably because the Gln-157 residue in the variant is protonated at a higher pH than glutamate. Although a number of threonine residues were highly conserved in the same region of several family-11 xylanases of

fungal origin and have their side chains highly solvent-exposed (23), one of the conserved residues was replaced with Glu-153 in XynI (see Fig. 1B). Unlike Glu-157, the carboxyl group of a closely neighboring residue Glu-153 in the thumb region protrudes into the solvent (see Fig. 5). The E153T variant did not differ from the wild-type in xylanase activity or pH optimum, suggesting that the Glu-153 residue was not related to optimum pH (Fig. 6).

In conclusion, this is the first report of the functional expression of *A. pullulans* xylanase in *P. pastoris* and the high secretion level using its own signal sequence. The mutational analysis of the recombinant xylanase based on the structural comparison of related xylanases suggested that Glu-157 as well as Asp-73 at the edge of the active site cleft play a significant role in its acidophilicity.

ACKNOWLEDGMENTS

This study was supported in part by The Iwatani Naoji Foundation's Research Grant, 2003.

REFERENCES

1. **Puls, J. and Schuseil, J.:** Chemistry of hemicelluloses: relationship between hemicellulose structure and enzymes required for hydrolysis, p. 1–27. *In* Coughlan, M. P. and Hazlewood, G. P. (ed.), Hemicellulose and hemicellulases. Portland Press, London (1993).
2. **Coughlan, M. P. and Hazlewood, G. P.:** β-1,4-D-Xylan-degrading enzyme systems: biochemistry, molecular biology and applications. Biotechnol. Appl. Biochem., **17**, 259–289 (1993).
3. **Henrissat, B.:** A classification of glycosyl hydrolases based on amino acid sequence similarities. Biochem. J., **280**, 309–316 (1991).
4. **Henrissat, B. and Bairoch, A.:** New families in the classification of glycosyl hydrolases based on amino acid sequence similarities. Biochem. J., **293**, 781–788 (1993).
5. **Ohta, K., Moriyama, S., Tanaka, H., Shige, T., and Akimoto, H.:** Purification and characterization of an acidophilic xylanase from *Aureobasidium pullulans* var. *melanigenum* and sequence analysis of the encoding gene. J. Biosci. Bioeng., **92**, 262–270 (2001).
6. **Li, X.-L. and Ljungdahl, L. G.:** Expression of *Aureobasidium pullulans xynA* in, and secretion of the xylanase from, *Saccharomyces cerevisiae*. Appl. Environ. Microbiol., **62**, 209–213 (1996).
7. **Cregg, J. M.:** Expression in the methylotrophic yeast *Pichia pastoris*, p. 157–191. *In* Fernandez, J. M. and Hoeffler, J. P. (ed.), Gene expression systems. Academic Press, New York (1999).
8. **Berrin, J.-G., Williamson, G., Puigserver, A., Chaix, J.-C., McLauchlan, W. R., and Juge, N.:** High-level production of recombinant fungal endo-β-1,4-xylanase in the methylotrophic yeast *Pichia pastoris*. Protein Express. Purif., **19**, 179–187 (2000).
9. **Sambrook, J. and Russell, D. W.:** Molecular cloning: a laboratory manual, 3rd ed. Cold Spring Harbor Laboratory Press, Cold Spring Harbor, New York (2001).
10. **Ho, S. N., Hunt, H. D., Horton, R. M., Pullen, J. K., and Pease, L. R.:** Site-directed mutagenesis by overlap extension using the polymerase chain reaction. Gene, **77**, 51–59 (1989).
11. **Miller, G. L.:** Use of dinitrosalicylic acid reagent for determination of reducing sugar. Anal. Chem., **31**, 426–428 (1959).
12. **Lowry, O. H., Rosebrough, N. J., Farr, A. L., and Randall, R. J.:** Protein measurment with the Folin phenol reagent. J. Biol. Chem., **193**, 265–275 (1951).
13. **Laemmli, U. K.:** Cleavage of structural proteins during the assembly of the head of bacteriophage T4. Nature, **227**, 680–685 (1970).
14. **Nakamura, T., Shitara, A., Matsuda, S., Matsuo, T., Suiko, M., and Ohta, K.:** Production, purification and properties of an endoinulinase of *Penicillium* sp. TN-88 that liberates inulotriose. J. Ferment. Bioeng., **84**, 313–318 (1997).
15. **Krengel, U. and Dijkstra, B. W.:** Three-dimensional structure of endo-1,4-β-xylanase I from *Aspergillus niger*: molecular basis for its low pH optimum. J. Mol. Biol., **263**, 70–78 (1996).
16. **Fushinobu, S., Ito, K., Konno, M., Wakagi, T., and Matsuzawa, H.:** Crystallographic and mutational analyses of an extremely acidophilic and acid-stable xylanase: biased distribution of acidic residues and importance of Asp37 for catalysis at low pH. Protein Eng., **11**, 1121–1128 (1998).
17. **Schwede, T., Kopp, J., Guex, N., and Peitsch, M. C.:** SWISS-MODEL: an automated protein homology-modeling server. Nucleic Acids Res., **31**, 3381–3385 (2003).
18. **Guex, N. and Peitsch, M. C.:** SWISS-MODEL and the Swiss-PdbViewer: an environment for comparative protein modeling. Electrophoresis, **18**, 2714–2723 (1997).
19. **Peitsch, M. C.:** Protein modeling by e-mail. Biotechnology (N.Y.), **13**, 658–660 (1995).
20. **Törrönen, A., Harkki, A., and Rouvinen, J.:** Three-dimensional structure of endo-1,4-β-xylanase II from *Trichoderma reesei*: two conformational states in the active site. EMBO J., **13**, 2493–2501 (1994).
21. **Li, X. L. and Ljungdahl, L. G.:** Cloning, sequencing, and regulation of a xylanase gene from the fungus *Aureobasidium pullulans* Y-2311-1. Appl. Environ. Microbiol., **60**, 3160–3166 (1994).
22. **Li, X. L., Zhang, Z. Q., Dean, J. F., Eriksson, K. E., and Ljungdahl, L. G.:** Purification and characterization of a new xylanase (APX-II) from the fungus *Aureobasidium pullulans* Y-2311-1. Appl. Environ. Microbiol., **59**, 3212–3218 (1993).
23. **Tahir, T. A., Berrin, J.-G., Flatman, R., Roussel, A., Roepstorff, P., Williamson, G., and Juge, N.:** Specific characterization of substrate and inhibitor binding sites of a glycosyl hydrolase family 11 xylanase from *Aspergillus niger*. J. Biol. Chem., **277**, 44035–44043 (2002).